JOURNAL OF EXPERIMENTAL AND THEORETICAL PHYSICS, 2024, Vol. 166, No. 2(8), pp. 161–168

ATOMS, MOLECULES, OPTICS

COHERENT PROPAGATION OF HALF-CYCLE LIGHT PULSE IN A THREE-LEVEL MEDIUM

R. M. Arkhipov[a,b*], A. V. Pakhomov[a], M. V. Arkhipov[a,b], N. N. Rozanov[a,b]

[a] *Saint Petersburg State University 199034, Saint Petersburg, Russia*
[b] *Ioffe Physical-Technical Institute of the Russian Academy of Sciences 194021, Saint Petersburg, Russia*
**e-mail: arkhipovrostislav@gmail.com*

Received March 04, 2024
Revised March 23, 2024
Accepted March 29, 2024

Abstract. Based on the numerical solution of Maxwell-Bloch equations, we study the dynamics of coherent propagation of unipolar, half-cycle, attosecond light pulse in a three-level resonantly absorbing medium. A comparison with the propagation of such pulse in a two-level medium is performed. It is shown that the pulse, which behaves like a 4π-pulse in a two-level medium, in a three-level medium behaves like a 6π-pulse and splits into three sub-pulses propagating at different velocities in the medium. The investigated phenomenon allows for a more detailed understanding of the still insufficiently studied dynamics of coherent propagation of half-cycle pulses in a resonant medium.

DOI: 10.31857/S004445102408e030

1. INTRODUCTION

Recently, there has been active research on the generation of unipolar half-cycle pulses containing a half-wave field of one polarity and possessing large electrical area, defined as [1–3]

$$S_E(\mathbf{r}) = \int_{-\infty}^{+\infty} E(\mathbf{r},t)dt. \quad (1)$$

Here E¿**r** t is the electric field strength, t is time, **r** is the radius vector. Interest in such pulses is related to the possibility of unidirectional action on charges, which enables rapid transfer of mechanical momentum to a charged particle, and consequently, such pulses can be used for ultrafast excitation of quantum systems, charge acceleration, and other applications [4, 5].

The electric area of such pulses is their important characteristic, as it satisfies the conservation rule in dissipative media in the one-dimensional case of plane wave propagation along the axis z: $dS_E/dz = 0$ [3, 6]. On the other hand, it determines the degree of impact on quantum systems if the pulse duration is less than the characteristic time associated with the ground state energy (orbital period of an electron in an atom) [7–14]. To date, several methods have been proposed for obtaining pulses that are close in shape to unipolar ones, having a pronounced half-wave field of one polarity [15–23]. A review of recent research in the field of obtaining such pulses and their applications can be found in reviews [4–6] and cited literature.

Although the question of existence and generation of such pulses has been analyzed in relatively detail (see reviews [4–6] and chapter in monograph [24]), coherent propagation of single-cycle and sub-cycle extremely short pulses in resonant media is insufficiently studied. Most previous studies of this issue were performed in the two-level approximation [25–33]. Taking into account a larger number of levels can, however, affect pulse dynamics in some cases [34] and lead to the formation of a complex photon echo pattern [35, 36]. Nevertheless, many studies show that the two-level model in some cases can adequately describe the interaction of an extremely short pulse with multilevel media [37, 38].

In paper [39], an analytical solution of the Maxwell-Bloch equations was found in the form of a unipolar self-induced transparency (SIT) soliton in the form of a hyperbolic secant. Subsequently, this soliton was discovered in numerical calculations during coherent propagation of an initially bipolar pulse in a two-level absorbing medium [27] and a three-level medium consisting of a mixture of absorbing and amplifying particles [40]. The existence of SIT solitons was shown in a multilevel medium in paper [41] through analytical solution of the sine-Gordon equation, see also reviews [42–45]. In several works analyzing coherent propagation of unipolar pulses in a medium, approximate analytical models were used [46–50], which, however, led to physically incorrect results, as the equations used did not satisfy the electric area conservation rule. A detailed analysis of the applicability limits of these approximations and their comparison with the area conservation rule are given in review [51].

In papers [52, 53] the dynamics of coherent propagation of a unipolar half-cycle pulse in a two-level absorbing medium was studied. It is shown that the field strength dynamics significantly depends on the initial electric area of the pulse. Thus, if the initial electric area of the pulse is such that it behaves like a 4π-pulse, then during propagation such pulse splits into a pair of 2π-like SIT pulses – during the pulse action the medium becomes excited, then returns to its initial state. Such behavior is similar to long pulses when the McCall and Hahn area theorem is satisfied [54–57].

In this work, based on numerical solution of the Maxwell-Bloch equations system, the dynamics of coherent propagation of a half-cycle attosecond pulse in a three-level resonantly absorbing medium is studied. It is shown that a pulse which acts as a 4π-pulse for a two-level medium behaves like a 6 -pulse in case of a three-level medium and splits into three sub- pulses. Each sub-pulse behaves like a 2π-pulse of SIT for each resonant transition.

2. THEORETICAL MODEL AND CONSIDERED SYSTEM

The analysis was carried out based on the well-known Maxwell-Bloch equations system for a three-level medium, which has the form [58]

$$\frac{\partial}{\partial t}\rho_{21} = -\rho_{21}/T_{21} - i\omega_{12}\rho_{21} - i\frac{d_{12}E}{\hbar}(\rho_{22} - \rho_{11}) - -i\frac{d_{13}E}{\hbar}\rho_{23} + i\frac{d_{23}E}{\hbar}\rho_{31}, \quad (2)$$

$$\frac{\partial}{\partial t}\rho_{32} = -\rho_{23}/T_{32} - i\omega_{23}\rho_{32} - i\frac{d_{23}E}{\hbar}(\rho_{33} - \rho_{22}) - -i\frac{d_{12}E}{\hbar}\rho_{31} + i\frac{d_{13}E}{\hbar}\rho_{21}, \quad (3)$$

$$\frac{\partial}{\partial t}\rho_{31} = -\rho_{31}/T_{31} - i\omega_{13}\rho_{31} - i\frac{d_{13}E}{\hbar}(\rho_{33} - \rho_{11}) - -i\frac{d_{12}E}{\hbar}\rho_{32} + i\frac{d_{23}E}{\hbar}\rho_{21}, \quad (4)$$

$$\frac{\partial}{\partial t}\rho_{11} = (1 - \rho_{11})/T_{11} + i\frac{d_{12}E}{\hbar}(\rho_{21} - \rho_{21}^*) - -i\frac{d_{13}E}{\hbar}(\rho_{13} - \rho_{13}^*), \quad (5)$$

$$\frac{\partial}{\partial t}\rho_{22} = -\rho_{22}/T_{22} - i\frac{d_{12}E}{\hbar}(\rho_{21} - \rho_{21}^*) - -i\frac{d_{23}E}{\hbar}(\rho_{23} - \rho_{23}^*), \quad (6)$$

$$\frac{\partial}{\partial t}\rho_{33} = -\rho_{33}\,/\,T_{33} + i\frac{d_{13}E}{\hbar}(\rho_{13} - \rho_{13}^*) + +i\frac{d_{23}E}{\hbar}(\rho_{23} - \rho_{23}^*), \quad (7)$$

$$P(z,t) = 2N_0 d_{12}\mathrm{Re}\,\rho_{12} + 2N_0 d_{13}\mathrm{Re}\,\rho_{13} + +2N_0 d_{23}\mathrm{Re}\,\rho_{32}, \quad (8)$$

$$\frac{\partial^2 E(z,t)}{\partial z^2} - \frac{1}{c^2}\frac{\partial^2 E(z,t)}{\partial t^2} = \frac{4\pi}{c^2}\frac{\partial^2 P(z,t)}{\partial t^2}. \quad (9)$$

In this system of equations $\rho_{11}, \rho_{22}, \rho_{33}$ – diagonal elements of the density matrix, representing the populations of the first, second, and third levels of the medium respectively, ρ_{21}, ρ_{32}, ρ_{31} – off-diagonal elements of the density matrix, determining the dynamics of medium polarization, ω_{12}, ω_{23}, ω_{13} – resonant transition frequencies, d_{12}, d_{13}, d_{23} – dipole moments of these transitions, $P(z,t)$ – polarization of medium, $E(z,t)$ – electric field, whose dynamics is described by wave equation (9). The equations also contain relaxation terms T_{ik}.

As initial conditions, a pulse in the form of a hyperbolic secant was launched into the medium from left to right from vacuum:

$$E(z = 0,t) = E_0\left(\frac{t - 6\tau}{\tau}\right). \quad (10)$$

For the pulse to behave like a 2π-pulse of SIT on the main transition 1–2 (if the medium is two-level), its amplitude must satisfy the relation [39]

$$E_{02} = \hbar/(d_{12}\tau). \quad (11)$$

The integration region had a length of $L = 15\lambda_0$. The medium was located in the center of the integration region between points $z_1 = 4\lambda_0$ and $z_2 = 12\lambda_0$. Numerical solution of the system

Table. Parameters of excitation pulses and medium

Pulse amplitude	$E_0 = 2.7 \cdot 10^5$ ESU
Duration of excitation pulses	$\tau = 380$ ac
Transition frequency 1–2 (transition wavelength)	$\omega_{12}= 2.69 \cdot 10^{15}$ rad/s ($\lambda_{12} = \lambda_0 = 700$ nm)
Dipole moment of transition 1–2	$d_{12} = 20$ D
Transition frequency 1–3	$\omega_{13}= 1.5\omega_{12}$
Dipole moment of transition 1–3 in hydrogen atom (transition wavelength)	$d_{13} = 1.5d_{12}$
Transition frequency 2–3	$\omega_{23}= \omega_{13}- \omega_{12}$
Dipole moment of transition 2–3	$d_{23} = 0$
Atom concentration	$N_0 = 2 \cdot 10^{20}$ cm^{-3}
Relaxation times	$T_{1k} = 100$ fs $T_{2k} = 30$ fs

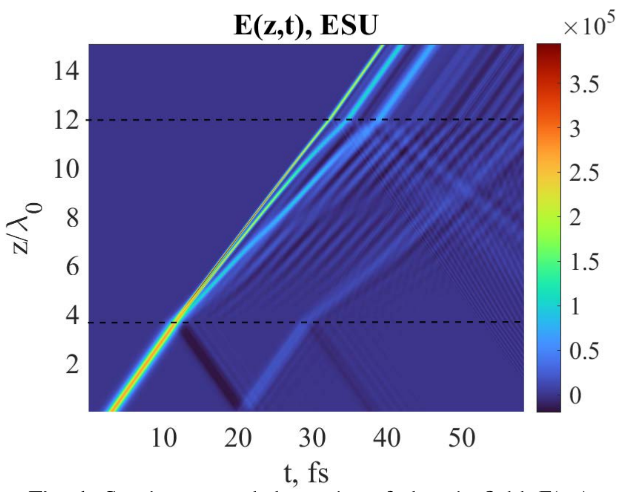

Fig. 1. Spatiotemporal dynamics of electric field $E(z,t)$ in three-level medium, whose boundaries are marked by dashed lines. The medium was located in the center of integration region between points $z_1 = 4\lambda_0$ and $z_2 = 12\lambda_0$

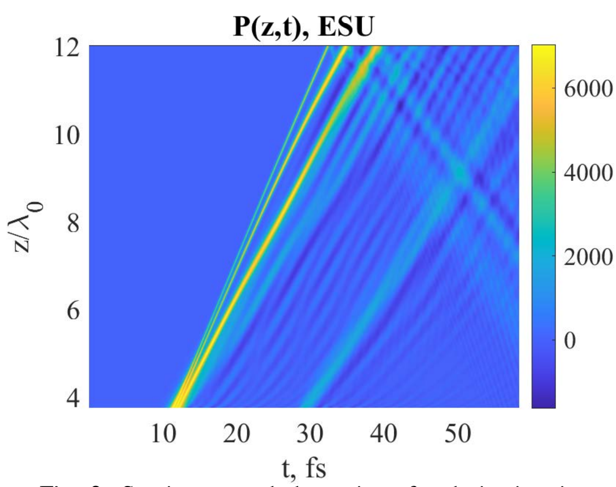

Fig. 2. Spatiotemporal dynamics of polarization in a three-level medium $P(z,t)$. The medium was located in the center of the integration region between points $z_1 = 4\lambda_0$ and $z_2 = 12\lambda_0$

of equations (2)–(9) was performed with initial condition (10). The parameters of the medium and pulse field are shown in the table. Note that in the considered example, the three-level medium has a so-called V-scheme of energy levels, i.e., resonant transitions $1 \to 2$ and $1 \to 3$ are allowed in the dipole approximation, while transition $2 \to 3$ is dipole-forbidden. The field amplitude value was chosen so that the pulse would act as a 4π-pulse for transition 1–2 of the two-level medium, $E_0 = 2E_{02}$.

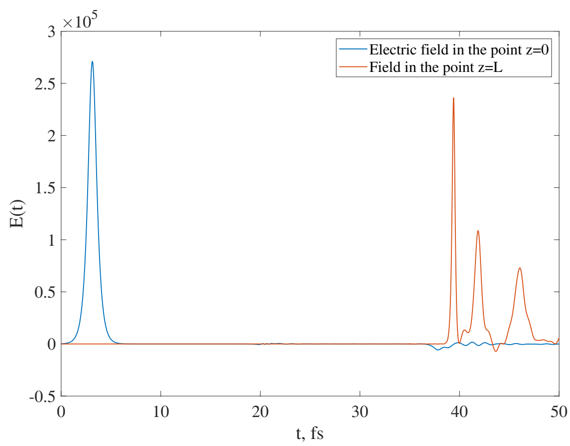

Fig. 3. Time dependence of the electric field $E(t)$ in the left part of the integration region $z = 0$ (blue curve on the left) and in the right part $z = L$ (orange line on the right)

3. RESULTS OF NUMERICAL MODELING AND DISCUSSION

Figs. 1 and 2 illustrate the spatiotemporal dynamics of the electric field of the pulse $E(z,t)$

and polarization of the three-level medium $P(z,t)$ respectively. The medium boundaries are marked with dashed lines in Fig. 1. It can be seen that the original pulse splits into three sub- pulses, each propagating at different speeds, so the sub-pulses gradually move away from each other. Thus, the original pulse, which would act as a 4π-pulse for a two-level medium, begins to behave like a 6π-pulse when a third level is added. After the pulses pass through, a polarization wave remains in the medium, which radiates after the passed pulses during the relaxation time T_2 (see Fig. 2).

The time dependence of the electric field at points $z = 0$ and $z = L$ for the case in Fig. 1 is shown in Fig. 3. Fig. 4 illustrates the time dependence of the population of the three medium levels at the beginning and end of the medium. It can be seen that the field intensity at the output of the medium consists of three sub-pulses. Also from Fig. 4, it is visible that the populations of each state return practically to their initial value after each sub-pulse, i.e., each sub-pulse acts like a 2π SIT pulse.

As calculations show for the case in Fig. 3, the electric area (1) of each of the three formed sub-pulses, calculated with the dimensionless coefficient, calculated with the dimensionless coefficient $2d_{12}/\hbar$, turns out to be approximately the same and equal to ≈1.3π. Thus, the initial 4π-pulse breaks down into sub-pulses in such a way that, taking into account other residual field oscillations after the three main sub-pulses at the output of the medium, the exact fulfillment of the electric area conservation rule is ensured.

It is interesting to note that a similar pattern with the splitting of the initial pulse into sub-pulses and close values of the electric area of each of them is observed at other values of the electric area of the initial incident pulse. For example, if the initial pulse has an area of 6π (again calculated with the dimensionless coefficient $2d_{12}/\hbar$), then after passing through the medium layer, it splits into five half-cycle sub-pulses of different amplitude and duration, but with approximately the same electric area ≈ ¿ π. If the initial pulse has an area of 2π, then at the output of the medium, one sub-pulse is formed with an electric area of ≈ 1.3π, followed by strongly pronounced slowly decaying alternating field oscillations, which at the same time have a total electric area of ≈ 0.7 .

The described pattern qualitatively persists at other values of dipole moments of allowed transitions in the three-level medium. For example, for the same medium parameters from the table, but under the condition $d_{12} = 1.5d_{13}$, numerical modeling showed the splitting of the initial 4π-pulse into two half-cycle sub-pulses with different amplitude and duration, but approximately equal values of electric area ≈ 1.8π (residual decaying os cillations of the field following the second sub-pulse had a total electric

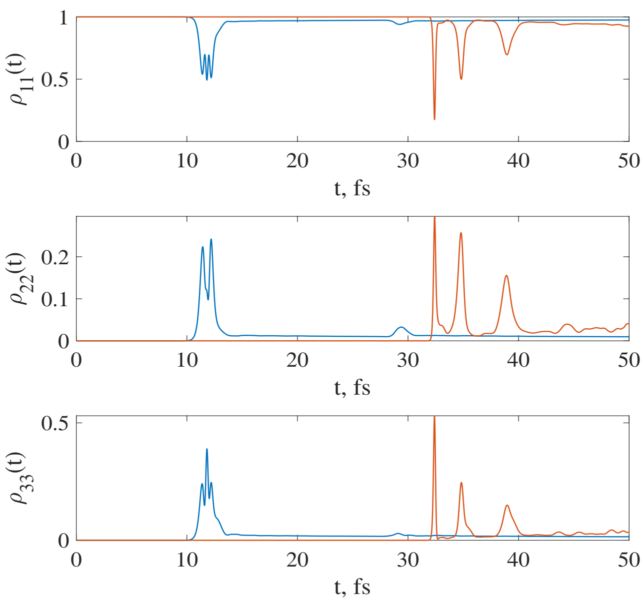

Fig. 4. Time dependencies of medium populations, blue lines – at the beginning of the medium (left curves), orange lines – at the end of the medium (right curves) formed sub-pulses

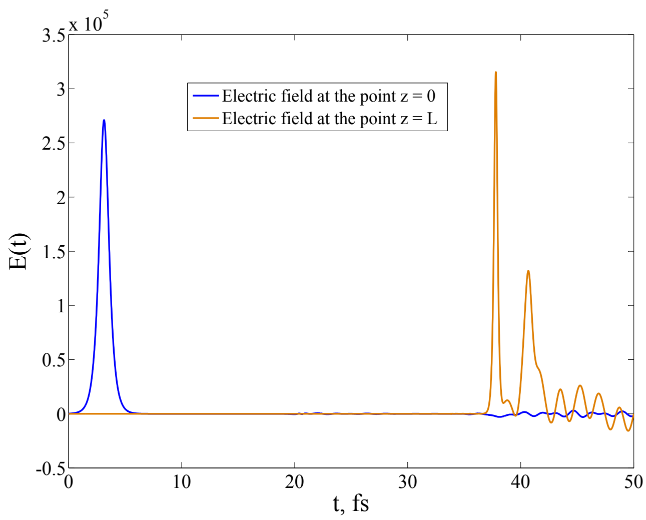

Fig. 5. Time dependence of the electric field $E(t)$ in the left part of the integration region $z = 0$ (blue curve on the left) and in the right part $z = L$ (orange line on the right); parameters are the same as in the table, except for the dipole moment $d_{13} = d_{12}/1.5$

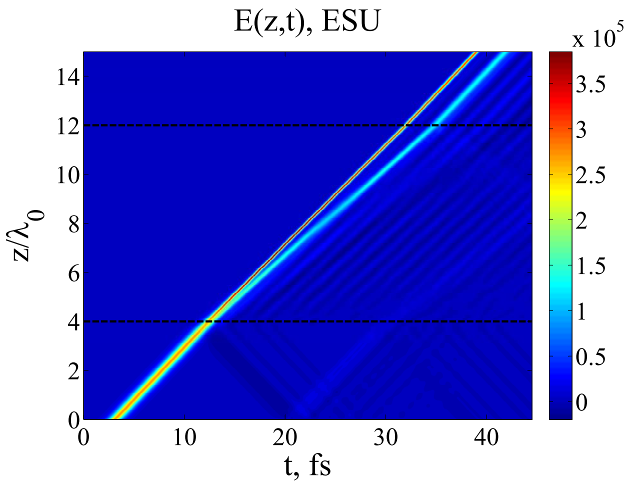

Fig. 6. Spatiotemporal dynamics of electric field E(z,t) in a three-level medium, whose boundaries are indicated by dashed lines. The medium was located in the center of the integration region between points $z_1 = 4\lambda_0$ and $z_2 = 12\lambda_0$; parameters are the same as in the table, except for the dipole moment $d_{13} = d_{12}/1.5$

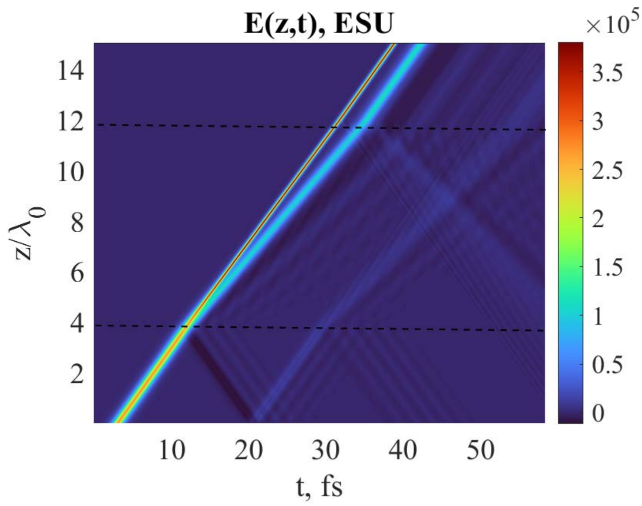

Fig. 8. Spatio-temporal dynamics of the electric field $E(z,t)$ in a two-level medium, whose boundaries are marked by dashed lines. The medium was located in the center of the integration region between points $z_1 = 4\lambda_0$ and $z_2 = 12\lambda_0$

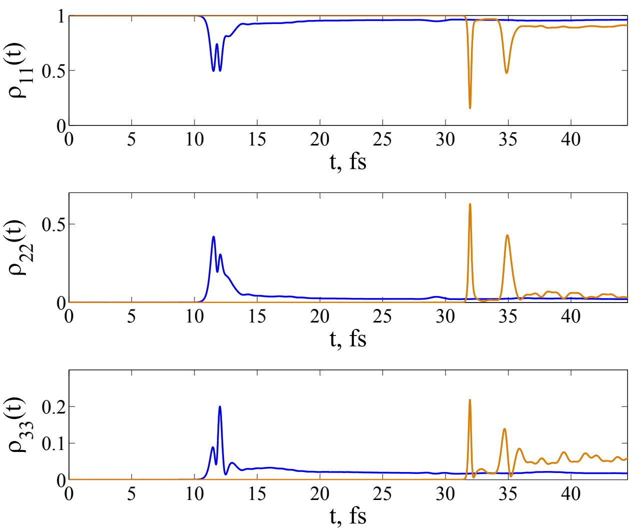

Fig. 7. Time dependencies of medium populations, blue lines – at the beginning of the medium (left curves), orange lines – at the end of the medium (right curves); parameters are the same as in the table, except for the dipole moment $d_{13} = d_{12}/1.5$

area $\approx 0.4\pi$). The corresponding spatial and temporal dependencies of the electric field and level populations are shown in Figs. 5–7.

It is not difficult to establish the physical cause of the observed splitting of the initial half-cycle pulse. It is analogous to the splitting of multi-cycle SIT pulses in a two-level medium. When adding a third level, the initial pulse, which was a 4π-pulse for the main 1–2 transition of the two-level medium, begins to act like a 2π-pulse for the 1–3 transition. As a result, for the "entire" medium, the pulse behaves like a 6π-pulse. During the propagation of such a pulse in the medium, as soon as the population difference for each transition returns to the ground state, complete absorption of the corresponding part of the pulse occurs, leading to its splitting. A similar mechanism leads to the splitting of long multi-cycle SIT pulses in a two-level medium [54–57].

4. COMPARISON WITH DYNAMICS IN A TWO-LEVEL MEDIUM

For comparison, similar dependencies of the electric field and state populations obtained from numerical solution of the Maxwell-Bloch equations system for a two-level medium [58] are shown in Figs. 8–10. In this case, the initial pulse behaves like a 4π-pulse and splits into a pair of 2π-like SIT pulses (see Figs. 8, 9). Other parameters are the same as in the table.

Thus, based on the presented numerical calculation results, it can be concluded that adding a third level leads to additional pulse splitting. However, the effect of splitting the initial pulse into sub-pulses, previously observed in calculations

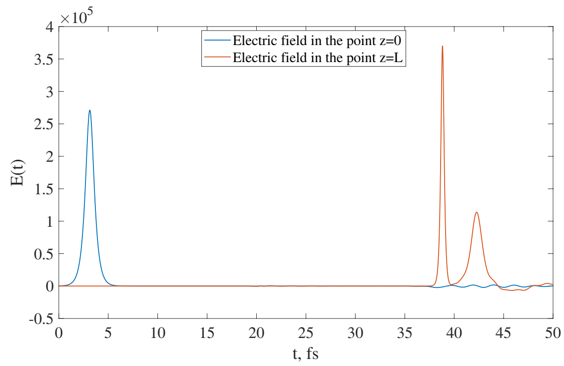

Fig. 9. Time dependence of the electric field $E(t)$ in the left part of the integration region $z = 0$ (blue curve on the left) and in the right part $z = L$ (orange line on the right)

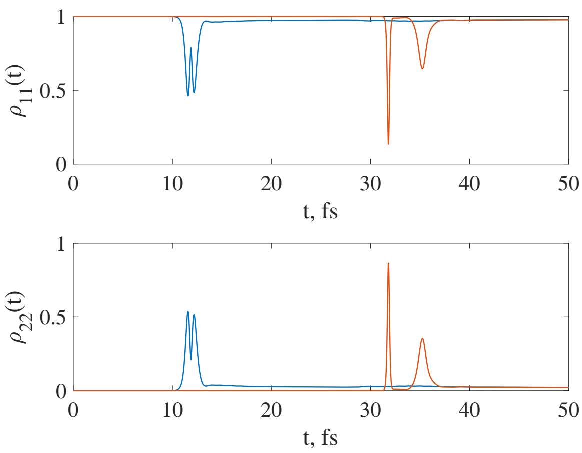

Fig. 10. Time dependencies of populations in a two-level medium, blue lines on the left – at the beginning of the medium, orange lines on the right – at the end of the medium

for a two-level medium [52, 53], persists in the multilevel medium as well.

5. CONCLUSIONS

Based on the numerical solution of the Maxwell-Bloch equations for a three-level medium, the dynamics of coherent propagation of a half-cycle attosecond pulse was studied. The amplitude and duration of the initial pulse were selected so that the pulse would act similar to a 4π-pulse for the main 1–2 transition in a two-level medium. It is shown that in a three-level medium, the pulse behaves like a 6π-pulse and splits into three 2π-like SIT pulses, each propagating at different speeds in the medium. Thus, the splitting of a half-cycle pulse, initially discovered in a two-level medium, persists in a three-level medium but has more complex dynamics – instead of splitting into a pair of subpulses, three subpulses emerge. The presented results help clarify the dynamics of coherent propagation of unipolar ultrashort pulses in multilevel resonant media, which is still insufficiently studied today. The investigated effect can be used for half-cycle pulse compression.

FUNDING

The research was carried out with financial support from the Russian Science Foundation within the framework of scientific projects 21-72-10028 (pulse dynamics in three-level medium) and 23-12-00012 (pulse dynamics in two-level medium).

REFERENCES

1. J. D. Jackson, *Classical Electrodynamics*, Mir, Moscow (1965) [J. D. Jackson, *Classical Electrodynamics*, Wiley, Hoboken, New York (1997)].

2. E. G. Bessonov, JETP **80,** 852 (1981) [E. G. Bessonov, Sov. Phys. JETP **53,** 433 (1981)].

3. N. N. Rosanov, Opt. Spectr. **107,** 761 (2009) [N. N. Rosanov, Opt. Spectr. **107,** 721 (2009)].

4. R. M. Arkhipov, M. V. Arkhipov, N. N. Rosanov, Quant. Electron. **50,** 801 (2020) [R. M. Arkhipov, M. V. Arkhipov, and N. N. Rosanov, Quant. Electron. **50,** 801 (2020)].

5. N. N. Rosanov, UFN **193,** 1127 (2023) [N. N. Rosanov, Phys. Usp. **66,** 1059 (2023)].

6. N. N. Rosanov, R. M. Arkhipov, M. V. Arkhipov, UFN **188,** 1347 (2018) [N. N. Romanov, R. M. Arkhipov, and M. V. Arkhipov, Phys. Usp. **61,** 1227 (2018)].

7. W. Pauli, *Handbuch der Physik*, Springer (1933).

8. A. B. Migdal, JETP **9,** 1163 (1939).

9. L. Schiff, *Quantum Mechanics*, McGraw-Hill (1968).

10. A. M. Dykhne, G. L. Yudin, UFN **125,** 377 (1978) [A. M. Dykhne and G. L. Yudin, Sov. Phys. Usp. **21,** 549 (1978)].

11. D. Dimitrovski, E. A. Solov'ev, and J. S. Briggs, Phys. Rev. A **72,** 043411 (2005).

12. A. S. Moskalenko, Z.-G. Zhu, and J. Berakdar, Phys. Rep. **672,** 1 (2017).

13. N. Rosanov, D. Tumakov, M. Arkhipov, and R. Arkhipov, Phys. Rev. A **104,** 063101 (2021).

14. A. Pakhomov, N. Rosanov, M. Arkhipov, and R. Arkhipov, JOSA B **41,** 46 (2024).

15. V. L. Ginzburg, S. I. Syrovatskii, UFN **87,** 65 (1965) [V. L. Ginzburg and S.I. Syrovatskii, Sov. Phys. Usp. **8,** 674 (1966)].

16. M. T. Hassan, T. T. Luu, A. Moulet, O. Raskazovskaya, P. Zhokhov, M. Garg, N. Karpowicz, A. M. Zheltikov, V. Pervak, F. Krausz, and E. Goulielmakis, Nature **530,** 66 (2016).

17. H.-C. Wu and J. Meyer-ter Vehn, Nature Photon. **6,** 304 (2012).

18. J. Xu, B. Shen, X. Zhang, Y. Shi, L. Ji, L. Zhang, T. Xu, W. Wang, X. Zhao, and Z. Xu, Sci. Rep. **8,** 2669 (2018).

19. I. E. Ilyakov, B. V. Shishkin, E. S. Efimenko, S. B. Bodrov, and M. I. Bakunov, Opt. Express **30,** 14978 (2022).

20. S. Wei, Y. Wang, X. Yan, and B. Eliasson, Phys. Rev. E **106,** 025203 (2022).

21. Q. Xin, Y. Wang, X. Yan, and B. Eliasson, Phys. Rev. E **107,** 035201 (2023).

22. A. V. Bogatskaya, E. A. Volkova, and A. M. Popov, Phys. Rev. E **104,** 025202 (2021).

23. M. Arkhipov, A. Pakhomov, R. Arkhipov, and N. Rosanov, Opt. Lett. **47,** 4637 (2023).

24. N. N. Rosanov, M. V. Arkhipov, R. M. Arkhipov, A. V. Pakhomov, *Collective monograph Terahertz Photonics*, eds. V. Ya. Panchenko, A. P. Shkurinov, Russian Academy of Sciences, Moscow (2023), p. 360.

25. X. Song, W. Yang, Z. Zeng, R. Li, and Z. Xu, Phys. Rev. A **82,** 053821 (2010).

26. S. Hughes, Phys. Rev. Lett. **81,** 3363 (1998).

27. V. P. Kalosha and J. Herrmann, Phys. Rev. Lett. **83,** 544 (1999).

28. A. V. Tarasishin, S. A. Magnitskii, V. A. Shuvaev, and A.M. Zheltikov, Opt. Express **8,** 452 (2001).

29. V. P. Kalosha and J. Herrmann, Phys. Rev. Lett. **83,** 544 (1999).

30. D. V. Novitsky, Phys. Rev. A **84,** 013817 (2011).

31. D. V. Novitsky, Phys. Rev. A **85,** 043813 (2012).

32. D. V. Novitsky, J. Phys. B: Atom. Mol. Opt. Phys. **47,** 095401 (2014).

33. D. V. Novitsky, Opt. Commun. **358,** 202 (2016).

34. J. Cheng and J. Zhou, Phys. Rev. A **67,** 041404 (2003).

35. A. Yu. Parkhomenko, S. V. Sazonov, JETP Lett. **67,** 887 (1998) [A. Y. Parkhomenko and S. V. Sazonov, JETP Lett. **67,** 934 (1998)].

36. S. V. Sazonov, A. F. Sobolevskii, JETP **123,** 919 (2003) [S. V. Sazonov and A. F. Sobolevskii, JETP **96,** 807 (2003)].

37. O. D. Mucke, T. Tritschler, M. Wegener, and U. Morgner, Phys. Rev. Lett. **87,** 057401 (2001).

38. A. Pakhomov, N. Rosanov, M. Arkhipov, and R. Arkhipov, JOSA B **41,** 46 (2024).

39. R. K. Bullough and F. Ahmad, Phys. Rev. Lett. **27,** 330 (1971).

40. N. V. Vysotina, N. N. Rozanov, V. E. Semenov, JETP Lett. **83,** 337 (2006) [N. V. Vysotina, N. N. Rozanov, and V. E. Semenov, JETP Lett. **83,** 279 (2006)].

41. A. Yu. Parkhomenko, S. V. Sazonov, JETP **114,** 1595 (1998) [A. Y. Parkhomenko and S. V. Sazonov, JETP **87,** 864 (1998)].

42. A. I. Maimistov, Quant. Electron. **30,** 287 (2000) [A. I. Maimistov, Quant. Electron. **30,** 287 (2000)].

43. A. I. Maimistov, Quant. Electron. **40,** 756 (2010) [A. I. Maimistov, Quant. Electron. **40,** 756 (2010)].

44. D. U. Mihalache, Roman. Rep. Phys. **69,** 403 (2017).

45. S. V. Sazonov, Opt. Spectr. **130,** 1846 (2022) [S. V. Sazonov, Opt. Spectr. **130,** 1573 (2022)].

46. E. M. Belenov, P. G. Kryukov, A. V. Nazarkin, A. N. Oraevskii, A. V. Uskov, JETP Lett. **47,** 442 (1988) [E. M. Belenov, P. G. Kryukov, A. V. Nazarkin, A. N. Oraevskii, and A. V. Uskov, JETP Lett. **47,** 523 (1988)].

47. E. M. Belenov, A. V. Nazarkin, JETP Lett. **51,** 252 (1990) [E. M. Belenov and A. V. Nazarkin, JETP Lett. **51,** 288 (1990)].

48. E. M. Belenov, A. V. Nazarkin, V. A. Ushchapovskii, JETP **100,** 762 (1991) [E. Belenov, A. Nazarkin, and V. Ushchapovskii, Sov. Phys. JETP **73,** 422 (1991)].

49. A. V. Bogatskaya, A. M. Popov, JETP Lett. **188,** 291 (2023) [A. V. Bogatskaya and A. M. Popov, JETP Lett. **118,** 296 (2023)].

50. A. V. Bogatskaya, E. A. Volkova, and A. M. Popov, Laser Phys. Lett. **21,** 015401 (2024).

51. A. V. Pakhomov, N. N. Rosanov, M. V. Arkhipov, R. M. Arkhipov, JETP Lett. **119,** 100 (2024) [A. V. Pakhomov, N. N. Rosanov, M. V. Arkhipov, and R.M. Arkhipov, JETP Lett. 119 (2024)].

52. R. M. Arkhipov, N. N. Rosanov, Opt. Spectr. **124,** 691 (2018) [R. M. Arkhipov and N.N. Rosanov, Opt. Spectr. **124,** 726 (2018)].

53. R. Arkhipov, M. Arkhipov, I. Babushkin, A. Pakhomov, and N. Rosanov, JOSA B **38,** 2004 (2021).

54. S. L. McCall and E.L. Hahn, Phys. Rev. **183,** 457 (1969).

55. P. G. Kryukov, V. S. Letokhov, Sov. Phys. Usp. **99,** 169 (1969) [P. G. Kryukov and V. S. Letokhov, Sov. Phys. Usp. **12,** 641 (1970)].

56. I. A. Poluektov, Yu. M. Popov, V. S. Roitberg, Sov. Phys. Usp. **114,** 97 (1974) [I. A. Poluektov, Yu. M. Popov, and V.S. Roitberg, Sov. Phys. Usp. **18,** 673 (1975)].

57. L. Allen, J. Eberly, *Optical Resonance and Two-Level Atoms*, Mir, Moscow (1978) [L. Allen and J. H. Eberly, *Optical Resonance and Two Level Atoms*, Wiley, New York (1975)].

58. A. Yariv, *Quantum Electronics*, Soviet Radio, Moscow (1980) [A. Yariv, *Quantum Electronics*, Wiley, New York (1975)].